

RELATIONSHIPS BETWEEN MICROSTRUCTURE AND MICROFISSURING IN ALLOY 718

R. G. Thompson
Materials Engineering
University of Alabama in Birmingham
Birmingham, AL 35294

Abstract

Microfissures which occur in the weld heat affected zone of alloy 718 can be a limiting factor in the material's weldability. Several studies have attempted to relate microfissuring susceptibility to processing conditions, microstructure, and/or heat-to-heat chemistry differences. These studies, however, are usually difficult to interpret due to the multiplicity of microstructure reactions which occurred in the various test groups. The present investigation studies the relationships between microstructure and microfissuring by isolating a particular microstructural feature and measuring microfissuring as a function of that feature. Results to date include the identification of a microstructure-microfissure sequence, microfissuring susceptibility as a function of grain size, and microfissuring susceptibility as a function of solution annealing time (Ni_3Nb - δ phase). This research effort is still in progress.

Introduction

Nickel base superalloys generally get their maximum strength from γ' [$\text{Ni}_3(\text{Al},\text{Ti})$] age hardening precipitates. The precipitation is very rapid and can lead to strain age cracking during welding. The strain age cracking problem limits weldability. Thus, the weldable superalloys are limited in their amount of Al and Ti and hence in their ultimate strength.

One method of increasing the ultimate strength of a superalloy while avoiding strain age cracking

is the addition of Nb (alias Cb). This produces γ' [Ni₃Nb] age hardening and, when used in conjunction with a limited amount of γ' , results in an increase in strength without strain age cracking problems. The γ'' does not lead to strain age cracking because its transformation kinetics are too slow to allow its formation during ordinary welding practice. This combination of γ' and γ'' strengthening was incorporated into the 718 type alloys.

Although the 718 alloy avoided the strain age cracking problem, it inherited a heat-affected zone (HAZ) microfissuring problem due to the Nb additions. Various studies were carried out to determine the cause of the microfissuring. These studies suggested that heat-to-heat chemistry differences had a strong influence on microfissuring susceptibility.^{2,3} They also showed that processing prior to welding² and heat treatment prior to welding^{2,4,5} both strongly influenced microfissuring susceptibility during welding. It was also strongly felt that grain size controlled microfissuring although experimental evidence was not conclusive.⁵

The present research builds on both prior experimental studies and practical experience to establish relationships between microstructure and microfissuring. These relationships are directly applicable to the wrought condition and, by judicious extrapolation, can be applied to cast and forged conditions as well. The research is divided into three sections which represent the three distinct experimental approaches used to study different microstructural features. Each section is capable of standing alone as a separate investigation. These three sections will be brought together in the Summary and Conclusions.

Microstructure-Microfissuring Sequence

Introduction/Procedure

Little was known of the sequence of events that

led to the formation of microfissures in alloy 718 when this investigation was initiated. It was believed that carbide⁴ or Laves^{2,5,6} phase liquation was involved in producing a zero ductility condition in the HAZ along grain boundaries. The hot ductility test using a Gleeble machine was widely used to determine this zero ductility condition for correlation with weld microfissuring.^{2,4}

The present study used a standard hot ductility test to generate typical hot ductility curves. A modified hot ductility test was also used in which samples were quenched to freeze the microstructure. A correlation was then made between the microstructure and hot ductility response as a function of the welding thermal cycle. A full description of this study has been published⁷ and the reader is referred to that expanded text for more details.

Results/Discussion

A typical hot ductility curve with corresponding microstructures is shown in Figure 1. These microstructure-ductility curves were produced for high temperature annealed, solution annealed, and age hardened conditions. Although these preweld heat treatments showed a wide range of microfissuring susceptibilities, they all showed the same microfissuring sequence. Figure 2 shows evolution of NbC into liquid and finally Laves phase. Figure 3 depicts our scheme of the microfissure formation in the presence of this intergranular liquid.

Several important conclusions can be drawn from the results of this study. First, results from microstructure-ductility curves typical of Figure 1 showed that no on-cooling ductility was lost until NbC melting started. Thus one prerequisite for microfissuring is the formation of intergranular liquid through NbC liquation. A second interesting point is that Laves phase precipitates from this

liquid. This would explain why many investigators associated microfissuring with Laves phase.

The Ni-Nb binary phase diagram supports these observations. It is found that a eutectic point exists at the temperature which NbC liquation occurs. The composition of this eutectic is about 50 w/o Nb. The Laves phase does not have this much Nb and thus could only cause liquation through a concentration of some low melting element such as sulfur. NbC on the other hand would act like a sink of pure Nb and could easily cause the eutectic composition.

The third point to be made is that preweld heat treatments altered microfissuring susceptibility. They do not, however, change the basic microfissuring mechanism of NbC liquation. Heat treating apparently affects the manner in which the intergranular liquid spreads across the grain boundaries. Figure 4 shows an intergranular fracture surface from alloy 718. By controlling the intergranular wetting of this liquid, perhaps the microfissuring of the alloy could be controlled.

Microfissuring-Grain Size Relationship

Introduction/Procedure

Grain size is so widely recognized as a contributing factor in microfissuring that it is often used to screen incoming 718 metal for weldability. Yet there is only one reference⁵ in the 718 literature which relates microfissuring to grain size and it is inconclusive. The purpose of the present study was to determine the relationship between grain size and microfissuring.

It was determined that a wide range of grain sizes could best be produced by using a high temperature grain growth anneal. The starting material was a single heat of 718 which was mill

processed into a uniform sheet with an average grain size of $\sim 10 \mu$ (ASTM #10). This grain size was progressively enlarged by holding to progressively longer times at $\sim 2160\text{F}$. Specimens were quenched from 2160F to prevent precipitation of unwanted secondary phases. It was felt that this treatment would minimize analytical variables such as heat-to-heat chemistry differences, impurity segregation, and secondary phases. It should be noted that the carbides were left undissolved since the thermal treatment was below the carbide liquation temperature.

The microfissuring susceptibility as a function of grain size was determined using a spot vareststraint test.⁸ In this test, microfissures were forced to occur around the periphery of a GTAW spot weld by straining the hot HAZ of the weld. The magnitude of microfissuring was correlated with grain size as shown in Figure 5.

Results/Discussion

As seen in Figure 5, microfissuring showed an almost linear dependence on grain size at all strain levels. The relative effect of grain size was to increase microfissuring 0.4% per micron ($1 \times 10^{-6}\text{m}$) increase in grain size. This represents substantial increases in microfissuring as the ASTM grain size number increases (Table 1).

TABLE 1

Microfissuring Dependence on Grain Size

ASTM Grain Size	Percentage Increase in Microfissuring above Baseline
9	baseline
7	5%
5	12%
3	38%
1	82%
00	175%

It is interesting to note that the relationship between microfissuring and grain size is independent of the strain level. It is also noteworthy that there is not a critical grain size below which microfissuring did not occur. Thus, if grain size is to be used as a weldability criterion, then it should be realized that such a criterion at best defines some microfissuring level of significance. It could not specify a microfissure, no-microfissure condition for a wide variety of welds.

Microfissure-Heat Treating Relationship

Introduction/Procedure

Heat treatments of interest in the 718 microfissuring problem are the solution anneal (1900-1700F) and age hardening (1400-1200F) treatments. Isothermal transformation diagrams are available in the literature which could be used to predict the precipitation reactions which might accompany these standard heat treatments. However, it was found that such diagrams are highly dependent on Nb segregation. Thus, published transformation diagrams are not generally applicable.

Given the above misgivings about predicted 718 transformations, certain generalities can be helpful when considering solution anneal and age hardening heat treatments. First, solution annealing usually is associated with reduced microfissuring while age hardening is usually associated with increased microfissuring. Solution annealing is also generally associated with Ni_3Nb (δ) precipitation while age hardening is associated with γ' , γ'' precipitation. The present work sought to identify some relationship between microfissuring and the precipitation of Ni_3Nb (δ) and γ' , γ'' .

Specimen preparation followed directly from the grain growth procedures already described. The grain growth procedure was carefully designed to eliminate secondary phases. It was thus uniquely

suited for the introduction of a specific second phase for analysis. A solution anneal of 1700F for 1 to 8 hours was used to produce a volume fraction range of $\text{Ni}_3\text{Nb}(\delta)$ precipitated into a 718 matrix of specific grain size. Samples thus prepared were tested in the spot vareststraint machine as previously described.

It should be possible to correlate microfissuring with the volume fraction of $\text{Ni}_3\text{Nb}(\delta)$. These volume fractions have not yet been measured so that microfissuring is plotted against solution annealing time as in Figure 6. Microfissuring versus either volume fraction of γ' , γ'' or hardness will also be presented in the final report but at this time the data is not yet ready.

Results/Discussion

Figure 6 shows that the solution anneal heat treatment was effective in reducing microfissuring only in the metal with large grain size. It is also evident that most of the beneficial effect is achieved in the first hour of heat treating. The last point of significance is that the reduction in microfissuring susceptibility was realized before $\text{Ni}_3\text{Nb}(\delta)$ precipitation was detected in the alloy.

The fact that microfissuring was reduced prior to $\text{Ni}_3\text{Nb}(\delta)$ precipitation is interesting. It might have been suspected that $\text{Ni}_3\text{Nb}(\delta)$ precipitation was the reason that solution annealing seemed to reduce microfissuring. That doesn't appear to be the case and other theories as to the mechanism of reduced microfissuring should be considered. One such theory is that of impurity or alloy segregation during the solution anneal heat treatment.

Summary

Microfissuring in wrought alloy 718 is due to the liquation of NbC and the subsequent intergranular liquid which is produced. If

sufficient strain is produced in the HAZ while the intergranular liquid is present, then microfissuring will result.

It is evident from Figure 5 that the magnitude of microfissuring in the HAZ is a function of both the strain level and the susceptibility of the microstructure to microfissure.

The susceptibility of the microstructure to microfissure can be easily understood if we assume that this susceptibility is defined by the distribution of the intergranular liquid as a function of temperature. Smith⁹ has defined the distribution of intergranular liquid in terms of the liquid's wetting angle. The boundaries seen in Figure 4 represent the case where liquid has not quite wet the grain boundary faces. This would be equivalent to a wetting angle slightly greater than zero. The HAZ would be most susceptible to microfissuring when the wetting angle reaches zero. One must also consider the temperature response of the wetting angle. The metal will be microfissure sensitive over the temperature range which the wetting angle remains zero during cooling from the weld. A large microfissure-sensitive temperature range translates into a long period of time over which cooling strains can concentrate in the HAZ and cause microfissuring.

Conclusions

1. NbC liquation is a prerequisite for microfissuring.
2. TiC has a higher stability temperature than does NbC and is not involved in the NbC liquation.
3. Laves phase is often associated with microfissuring because it precipitates from the Nb-rich intergranular liquid onto the microfissure fracture surfaces.

4. Increasing grain size increases microfissure susceptibility at the rate of 0.4% per micron (1×10^{-6} m) increase in grain size.
5. The grain size effect is independent of the applied strain.
6. Solution annealing significantly reduces microfissuring only in metal with a large grain size.
7. The major reduction of microfissuring during solution anneals occurs during the first 30 to 60 minutes at 1700F.
8. The observed reduction in microfissuring during solution annealing does not appear to be related to the $\text{Ni}_3\text{Nb}(\delta)$ precipitation which often accompanies that heat treatment.
9. It was found that age hardening increased microfissuring, but it has not yet been determined if the increased microfissuring correlates with matrix hardness.

References

1. Eiselstein, H. S. 1965. Metallurgy of a columbium-hardened and nickel-chromium-iron alloy. ADVANCES IN TECHNOLOGY OF STAINLESS STEEL AND RELATED ALLOYS, ASTM STP 369:62-79.
2. Thompson, E. G. 1969. Hot cracking studies of alloy 718 weld heat-affected zone. Welding Journal 48 (2):70-s to 79-s.
3. Morrison, T. J., Shira, C. S., and Weisenberg, L.A. 1969. Effect of Minor Elements on Alloy 718 Weld Microfissuring. Effects of Minor Elements on the Weldability of High-Nickel Alloys. Welding Research Council, N.Y., N.Y.:47.

4. Duvall, D. S., and Owczarski, W. A. 1967. Further heat-affected zone studies in heat resistant nickel alloys. Welding Journal 46(9):423-s to 432-s.
5. Valdez, P. J. and Steinman, J. B. 1969. Effect of Composition and Thermal Treatments on the Weldability of Nickel-Base 718 Alloy. Effects of Minor Elements on the Weldability of High-Nickel Alloys. Welding Research Council. N.Y., N.Y.:93.
6. Vincent, E. R. 1980. The microstructure of welds in Inconel 718. Department of Physics, University of Bristol, United Kingdom.
7. Thompson, R. G. and Genculu, S. 1983. Microstructural Evolution in the HAZ of Inconel 718 and Correlation with the Hot Ductility Test. Welding Journal 62(12):337-s to 345-s.
8. Savage, W. F., Nippes, E. F. and Goodwin, G. W. 1977. Effects of Minor Elements on Hot Cracking Tendencies of Inconel 600. Welding Journal 56:245-s.
9. Smith, C. S., 1948. Grains, phases and interfaces: an interpretation of microstructure. Trans. A.I.M.M.E. 175:175.

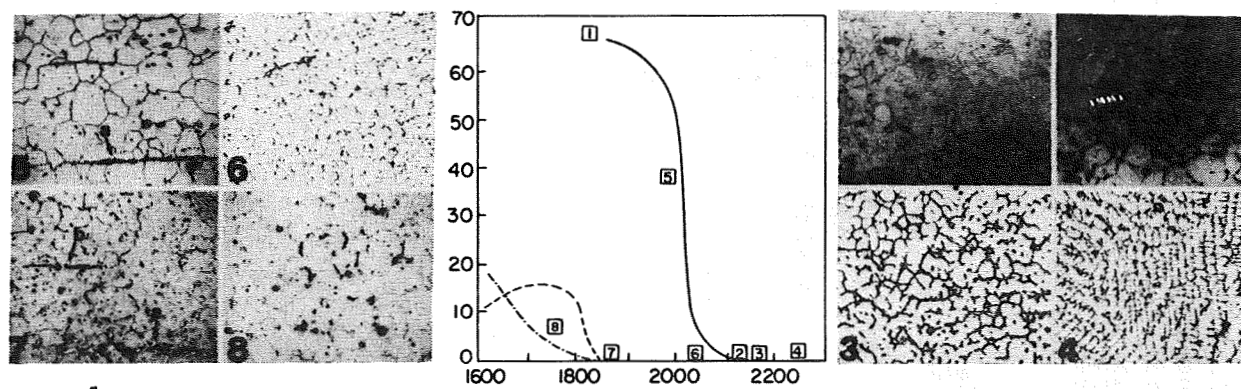
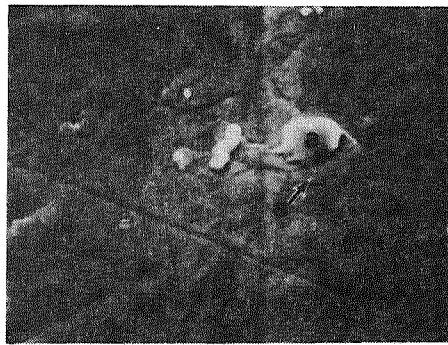


FIGURE 1.
MICROSTRUCTURAL EVOLUTION IN AS RECEIVED 718 DURING HOT DUCTILITY TEST.



a - NbC particle

d - Laves phase precipitation from liquid e

e - Liquid from liquated NbC particle

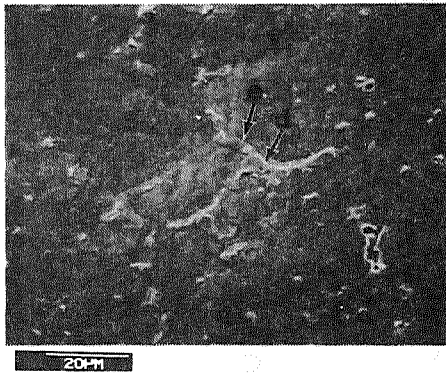
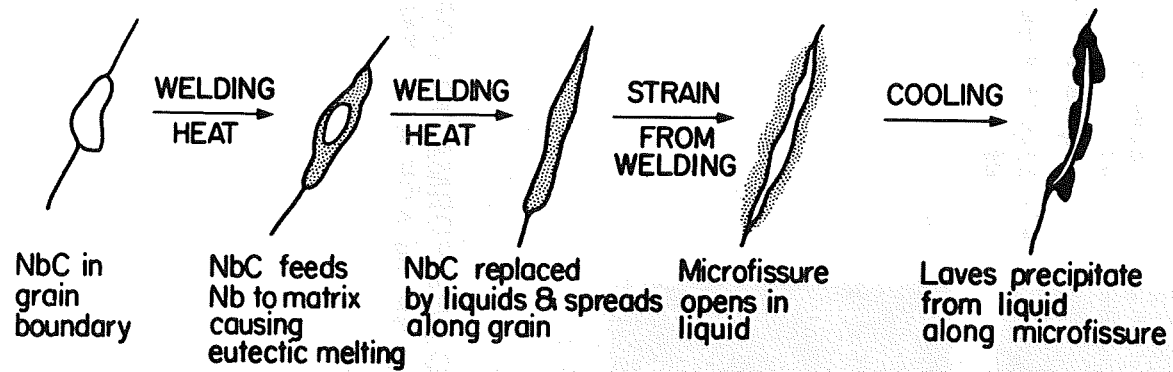


Figure 2

DISSOLUTION OF NbC AND FORMATION OF INTERCRANULAR PHASE IN AGE HARDENED 718.



Microstructure - Microfissure Sequence

FIGURE 3

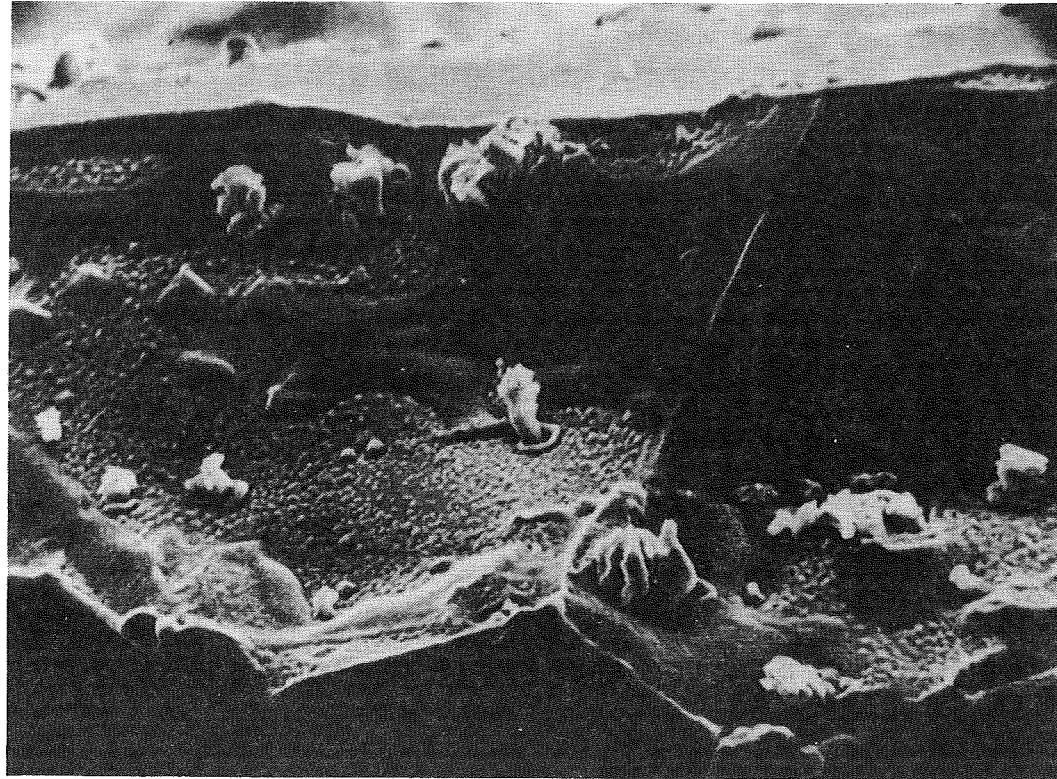


FIGURE 4
FRACTURE SURFACE - 2200°F, 500X

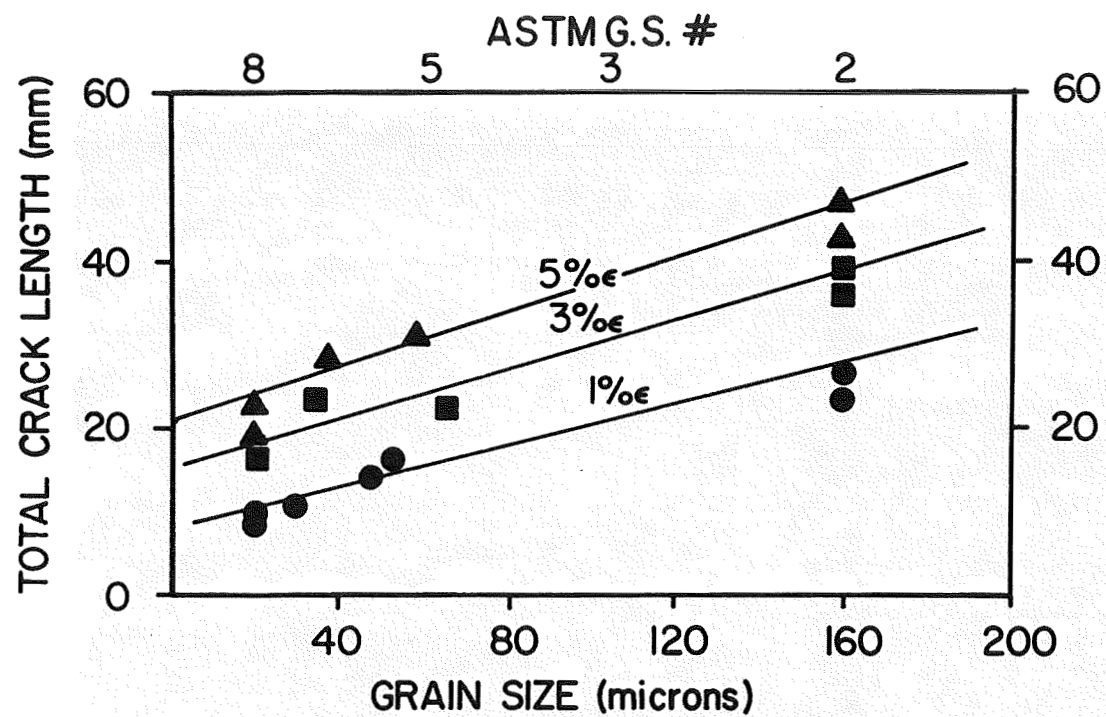
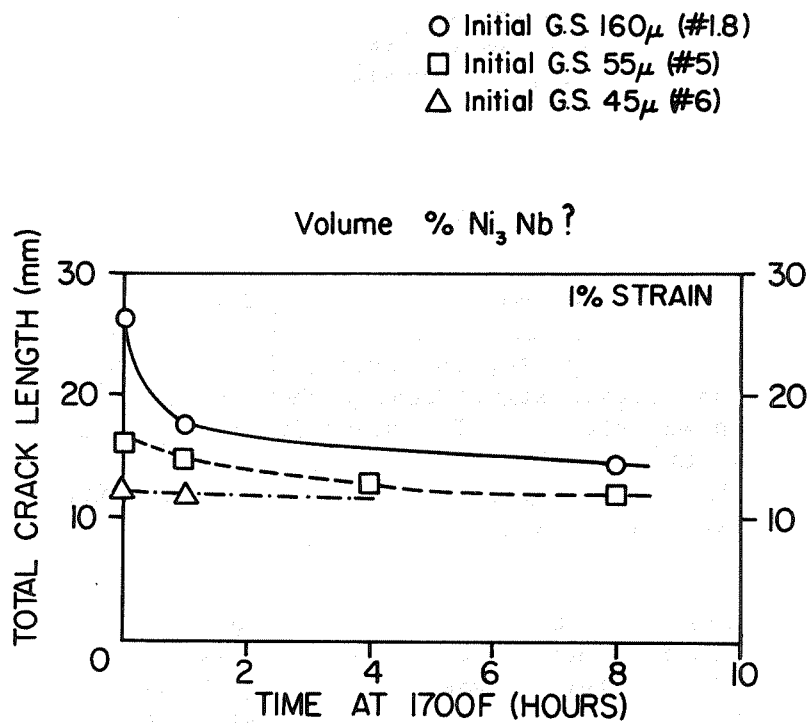


FIGURE 5 Effect of Grain Size on Total HAZ Crack Length in the Spot Varestraint Test



Effect of Annealing Time at 1700F on
Microfissuring Susceptibility
FIGURE 6